NASA SP-8019

NASA SPACE VEHICLE DESIGN CRITERIA (STRUCTURES)

BUCKLING OF THIN-WALLED TRUNCATED CONES

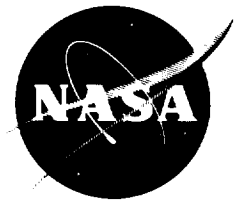

SEPTEMBER 1968

NATIONAL AERONAUTICS AND SPACE ADMINISTRATION

FOREWORD

NASA experience has indicated a need for uniform criteria for the design of space vehicles. Accordingly, criteria are being developed in the following areas of technology:

Environment

Structures

Guidance and Control

Chemical Propulsion.

Individual components of this work will be issued as separate monographs as soon as they are completed. A list of all previously issued monographs in this series can be found on the last page of this document.

These monographs are to be regarded as guides to design and not as NASA requirements, except as may be specified in formal project specifications. It is expected, however, that the criteria sections of these documents, revised as experience may indicate to be desirable, eventually will become uniform design requirements for NASA space vehicles.

This monograph was prepared under the cognizance of the Langley Research Center. The Task Manager was A. L. Braslow. The authors were V. I. Weingarten and P. Seide of the University of Southern California. A number of other individuals assisted in developing the material and reviewing the drafts. In particular, the significant contributions made by E. H. Baker of North American Rockwell Corporation; C. D. Babcock, Jr., of California Institute of Technology; R. F. Crawford of Astro Research Corporation; J. B. Glassco of McDonnell Douglas Corporation; A. Kaplan of TRW Systems; M. H. Kural of Lockheed Missiles & Space Company; J. Mayers of Stanford University; and J. P. Peterson of NASA Langley Research Center are hereby acknowledged.

Comments concerning the technical content of these monographs will be welcomed by the National Aeronautics and Space Administration, Office of Advanced Research and Technology (Code RVA), Washington, D.C. 20546.

September 1968

For sale by the Clearinghouse for Federal Scientific and Technical Information
Springfield, Virginia 22151 – Price $3.00

CONTENTS

SYMBOLS

A_r	cross-sectional area of ring
D	wall flexural stiffness per unit width, $\frac{Et^3}{12(1-\mu^2)}$
E	Young's modulus
$\bar{E}$	equivalent Young's modulus for isotropic sandwich shell
E_f	Young's modulus of face sheet of sandwich shell
E_R	reduced modulus
E_r	Young's modulus of ring
E_s, E_θ	Young's moduli of orthotropic material in the s and θ directions, respectively
$\bar{E}_s, \bar{E}_\theta$	equivalent Young's moduli of orthotropic material in the s and θ directions, respectively
E_{sec}	secant modulus for uniaxial stress-strain curve
E_{tan}	tangent modulus for uniaxial stress-strain curve
E_z	Young's modulus of sandwich core in direction perpendicular to face sheet of sandwich shell
E_1, E_2	Young's moduli of the face sheets for isotropic sandwich shell
e_r	distance of the centroid of the ring-shell combination from the middle surface
f	ratio of minimum to maximum principal compressive stress in face sheets
G	shear modulus
$\bar{G}$	equivalent shear modulus
G_{sz}	shear modulus of core of sandwich wall in s-z plane
h	depth of sandwich wall measured between centroids of two face sheets
I_r	moment of inertia of ring cross-section about centroidal axis of ring
L_o	ring spacing measured along cone generator
ℓ, L	axial and slant length of cone, respectively
M	bending moment on cone
M_{cr}	critical bending moment on cone
M_{press}	bending moment at collapse of a pressurized cone
n	number of buckle waves in the circumferential direction

P axial load on cone

P_{cr} critical axial load on cone

p applied uniform internal or external hydrostatic pressure

p_{cr} critical hydrostatic pressure

R_b ratio of bending moment on cone subjected to more than one type of loading to the allowable bending moment for the cone when subjected only to bending

R_c ratio of axial load on cone subjected to more than one type of loading to the allowable axial load for the cone when subjected only to axial compression

R_p ratio of external pressure on cone subjected to more than one type of loading to the allowable external pressure for the cone when subjected only to hydrostatic pressure

R_t ratio of torsional moment on cone subjected to more than one type of loading to the allowable torsional moment for the cone when subjected only to torsion.

r equivalent cylindrical shell radius [see eq. (11a)]

r_1 radius of small end of the cone

r_2 radius of large end of the cone

S cell size of honeycomb core

s distance along cone generator measured from vertex of cone

s_1 distance along cone generator measured from vertex of cone to small end of cone

T torsional moment on cone

T_{cr} critical torsional moment on cone

t skin thickness of isotropic cone

$\bar{t}$ effective skin thickness of isotropic sandwich cone

t_f thickness of one face sheet of sandwich cone having equal thickness sheets

t_1, t_2 face sheet thicknesses for sandwich construction having sheets of unequal thickness

z coordinate normal to the face sheet of sandwich shell

$\tilde{z}_r$ distance of the centroid of the ring cross-section from the shell middle surface

α semivertex angle of cone

γ correlation factor to account for difference between classical theory and predicted instability loads

$\Delta\gamma$ increase in buckling correlation factor due to internal pressure

δ ratio of core density of honeycomb sandwich plate to density of face sheet of sandwich plate

η plasticity reduction factor

η_o ring-geometry parameter

θ coordinate in the circumferential direction

μ Poisson's ratio

μ_s, μ_θ Poisson's ratios associated with stretching of an orthotropic material in the s and θ directions, respectively

$\bar{\mu}_s, \bar{\mu}_\theta$ equivalent Poisson's ratios in the s and θ directions, respectively

$\bar{\rho}$ average radius of curvature of cone, $\frac{r_1 + r_2}{2 \cos \alpha}$

ρ_1 radius of curvature at small end of cone, $\frac{r_1}{\cos \alpha}$

ρ_2 radius of curvature at large end of cone, $\frac{r_2}{\cos \alpha}$

σ_{max} maximum membrane compressive stress

σ_N normal stress

σ_s local failure stress

τ_{cr} critical shear stress

BUCKLING OF THIN-WALLED TRUNCATED CONES

1. INTRODUCTION

Structural components are said to be unstable under static loading when infinitesimal load increases or other small disturbances induce the structure to change from one equilibrium configuration to another of a different character. For some structures and loadings, the two configurations may differ only slightly, and large changes of shape may therefore develop gradually with successive increases in load. In this case, the load at which initial buckling occurs is not really significant. Generally, a more significant load is the ultimate load of the structure, which may be reached when the material fails plastically or when the structure collapses. For other structures and loadings, however, the change from one equilibrium configuration to another may be of considerable magnitude, and the transition is extremely rapid. This rapid initial buckling usually causes the structure to lose its capacity to sustain further increases in load, or it causes such large deformations that the structure is rendered unsafe for further use.

The primary design problem is the prevention of buckling which leads to undesirable configurations – in particular, collapse. The magnitude of the critical static load of a structure generally depends on its geometric proportions, the manner in which it is stiffened, the manner in which it is supported, the bending and extensional stiffnesses of its various components, or other reasonably well-defined characteristics. For thin-walled shell structures, less certain characteristics, such as small deviations of the structure from its nominal unloaded shape, may also have quite important effects on the load at which buckling will occur. Other factors that affect buckling, such as cutouts, nonuniform stiffnesses, and variation of loading with time, are not considered in this monograph.

This monograph recommends practices for predicting buckling of uniform stiffened and unstiffened circular conical shells under various types of static loading and suggests procedures that yield estimates of static buckling loads which are considered to be conservative. The buckling of cylindrical shells and shells of double curvature will be treated in separate monographs.

Estimation of design loads for buckling involves the use of the ultimate design factor. Considerations involved in selecting the numerical value of this factor will be presented in another monograph.

2. STATE OF THE ART

Many studies have been conducted of the buckling of conical shells under various loading conditions. Knowledge of the elastic stability of conical shells, however, is not as extensive as that of cylindrical shells. While the behavior of the two types of shells appears to be similar, significant differences in experimental results remain unexplained. Frequently, there are insufficient data to cover the wide range of conical-shell geometric parameters. In addition, some important loading cases and the effects of edge conditions remain to be studied. These problems can be treated by digital computers. A program for shells with uniform wall stiffnesses under axisymmetric loading is given in reference 1; reference 2 provides a program for shells with axisymmetric geometric properties but asymmetric loadings.

In spite of these handicaps, design criteria can be obtained by combining available theoretical and experimental data on conical shells with experience gained from studies of cylindrical shells. The designer is, however, advised to be alert to new developments in shell-stability analysis to put improved procedures to immediate use. The recommendations given in this monograph will be modified as more theoretical and test data become available.

3. CRITERIA

3.1 General

Structural components consisting of thin, curved isotropic or composite sheet, with or without stiffening, shall be so designed that (1) buckling that results in collapse of the structural components will not occur from the application of design loads, and (2) buckling deformations resulting from limit loads will not be so large as to impair the function of the structural component or nearby components nor so large as to produce undesirable changes in loading.

3.2 Guides for Compliance

Design loads for buckling are considered to be any combination of ground or flight loads, including loads resulting from temperature changes, that cause compressive inplane stresses (multiplied by the ultimate design factor) and any load or load combination tending to alleviate buckling (not multiplied by the ultimate design factor). For example, external pressure loads or torsional loads should be increased by the design factor, but internal pressure loads should not.

Suitable tests are required of representative structures under conditions simulating the design loads when minimum weight is a dominant factor or when cutouts, elastic end supports, or other special problems occur in the design.

4. RECOMMENDED PRACTICES

4.1 Scope

Within the limitations imposed by the state of the art, acceptable procedures for the estimation of critical loads on conical shells are described in this section. The important problems are indicated and the source of the procedures and their limitations are discussed. Where the recommended procedure is complex and is suitably defined in all its detail in a readily available reference, it is merely outlined. Where practicable, a summary of the procedure is given.

4.2 Isotropic Conical Shells

The following pages present recommended design procedures for isotropic conical shells under such loading conditions as axial compression, bending, uniform hydrostatic pressure, and torsion, along with those of combined loads.

4.2.1 Axial Compression

Buckling and collapse loads coincide for conical shells under axial compression. There is considerable disagreement between experimental loads and the loads predicted by theory. These discrepancies have been attributed to the effects of imperfections of the structure and of edge-support conditions different from those assumed in the analysis, as well as to shortcomings of the small-deflection theory used.

A theoretical analysis (ref. 3) indicates that the critical axial load for long conical shells can be expressed as

$$P_{cr} = \gamma \frac{2\pi E t^2 \cos^2 \alpha}{\sqrt{3(1-\mu^2)}} \tag{1}$$

with the theoretical value of γ equal to unity. Experiments (refs. 4 and 5) indicate that within the range of the geometries of the tested specimens there is no apparent effect of conical-shell geometry on the correlation factor. Therefore, γ can be taken as a constant. At present, γ is recommended to be taken as

$$\gamma = 0.33 \quad (10^\circ < \alpha < 75^\circ) \tag{2}$$

which gives a lower bound to the experimental data. Buckling-load coefficients for cone semivertex angles greater than 75° must be verified by test because experimental data are not available in this range. Compressive buckling coefficients for equivalent cylindrical shells can be used for cones with semivertex angles less than 10°, for which little or no experimental data are available. The recommended equivalent cylinder has the same wall thickness as the cone and a length and radius equal to the slant length, L, and average radius of curvature, $\bar{\rho}$, of the cone, respectively.

No studies have been published on the compressive buckling of conical shells in the yield region. Because the nominal stress level in a conical shell varies along its length, the effects of plasticity in conical shells are likely to differ from those in cylindrical shells. A conservative estimate of plasticity effects in conical shells could be obtained, however, if the reduction factors for cylindrical shells are used. The value E in equation (1) should be replaced by the value ηE (ref. 6) where

$$\eta = \frac{\left(E_{sec} E_{tan}\right)^{\frac{1}{2}}}{E} \tag{3}$$

The secant and tangent moduli should correspond to the maximum membrane compressive stress

$$\sigma_{max} = \frac{P}{2\pi\rho_1 t \cos^2 \alpha} \tag{4}$$

4.2.2 Bending

For unpressurized conical shells in bending, buckling and collapse loads coincide. Although no theoretical results are available for this problem, a load-correlation parameter is suggested by the following reasoning.

Reference 7 shows that in theory the predicted buckle wavelength for cylinders in bending is small, and that the maximum compressive bending stress should be approximately equal to the critical axial compressive stress. For conical shells in axial compression, reference 5 indicates that the critical local meridional stress is equal to the critical compressive stress of a cylinder having the same wall thickness and the same

local radius of curvature. It is also known that stresses in cones under bending decrease in the longitudinal direction at a much faster rate than do the corresponding stresses in axially compressed cones.

It therefore appears reasonable to hypothesize that the small-deflection theory for conical shells in bending would predict that buckling occurs when the maximum compressive stress at or near the small end of the cone is equal to the critical compressive stress of a cylinder having the same wall thickness and the same local radius of curvature. The buckling moment can thus be assumed to be given by

$$M_{cr} = \gamma \frac{\pi E t^2 r_1 \cos^2 \alpha}{\left[3\,(1-\mu^2)\right]^{\frac{1}{2}}} \tag{5}$$

with the theoretical value of γ equal to unity.

In the only available experimental study (ref. 8), use is made of a number of specimens about equal to the number of conical shells subjected to axial compression, but the study covers a much more restricted range of geometrical parameters. The experimental data appear to verify the load-correlation parameter given by equation (5) and indicate that the coefficients for conical shells in bending are larger than those for axially compressed conical shells. This is also the case for cylindrical shells. The data are insufficient to indicate any other trends. It is therefore recommended that the coefficient γ be taken as the constant value

$$\gamma = 0.41 \qquad (10^\circ < \alpha < 60^\circ) \tag{6}$$

Buckling-load coefficients for cone semivertex angles greater than 60° must be verified by test because experimental data are not available in this range. Buckling coefficients for equivalent cylindrical shells in bending can be used with semivertex angles less than 10°. For conical shells for which plasticity effects are significant, the correction suggested for conical shells in axial compression may be used; i.e., E in equation (5) may be replaced by ηE, given by equation (3).

4.2.3 Uniform Hydrostatic Pressure

The theoretical buckling pressure of a conical shell which buckles into several circumferential waves ($n > 2$) can be expressed (ref. 9) in the approximate form

$$p_{cr} = \frac{0.92 E \gamma}{\left(\frac{L}{\bar{\rho}}\right)\left(\frac{\bar{\rho}}{t}\right)^{\frac{5}{2}}} \tag{7}$$

The theoretical value of γ is greater than unity and is insensitive to geometric parameters other than the ratio of the end radii of the conical shell for a wide range of cone geometries. With γ equal to unity, equation (7) yields a buckling pressure identical to the approximate hydrostatic buckling pressure of a circular cylindrical shell (ref. 10) with a length equal to the slant length of the conical shell, with a radius equal to the average radius of curvature $\bar{\rho}$ of the conical shell, and with the same wall thickness. Experiments (refs. 11 and 12) show a relatively wide scatter band for the value of γ but indicate that the constant value

$$\gamma = 0.75 \tag{8}$$

should provide a lower bound for the available data.

For conical shells which buckle in the plastic range, the plasticity correction for moderate-length cylindrical shells may be used for the range of the conical shell geometries considered. The procedure here is to replace Young's modulus E in equation (7) by ηE (ref. 6), where

$$\eta = \frac{E_{sec}}{E} \left(\frac{E_{tan}}{E_{sec}}\right)^{\frac{1}{4}} \left(\frac{1}{4} + \frac{3}{4}\frac{E_{tan}}{E_{sec}}\right)^{\frac{1}{2}} \tag{9}$$

and the moduli correspond to the maximum circumferential compressive stress at the large end of the conical shell:

$$\sigma_{max} = p_{cr}\left(\frac{\rho_2}{t}\right) \tag{10}$$

Plasticity factors for the biaxial-stress state of hydrostatic pressure are unavailable. For lack of better information, the plasticity factor given by equation (9) may be used.

4.2.4 Torsion

An approximate equation for the critical torque of a conical shell (ref. 13) is

$$T_{cr} = 52.8\gamma D\left(\frac{t}{\ell}\right)^{\frac{1}{2}}\left(\frac{r}{t}\right)^{\frac{5}{4}} \tag{11}$$

where

$$r = r_2 \cos \alpha \left\{ 1 + \left[\frac{1}{2} \left(1 + \frac{r_2}{r_1} \right) \right]^{\frac{1}{2}} - \left[\frac{1}{2} \left(1 + \frac{r_2}{r_1} \right) \right]^{-\frac{1}{2}} \right\} \frac{r_1}{r_2} \tag{11a}$$

The variation of the bracketed function with the cone taper ratio $1 - \frac{r_1}{r_2}$ is plotted in figure 1. The theoretical value of γ is unity.

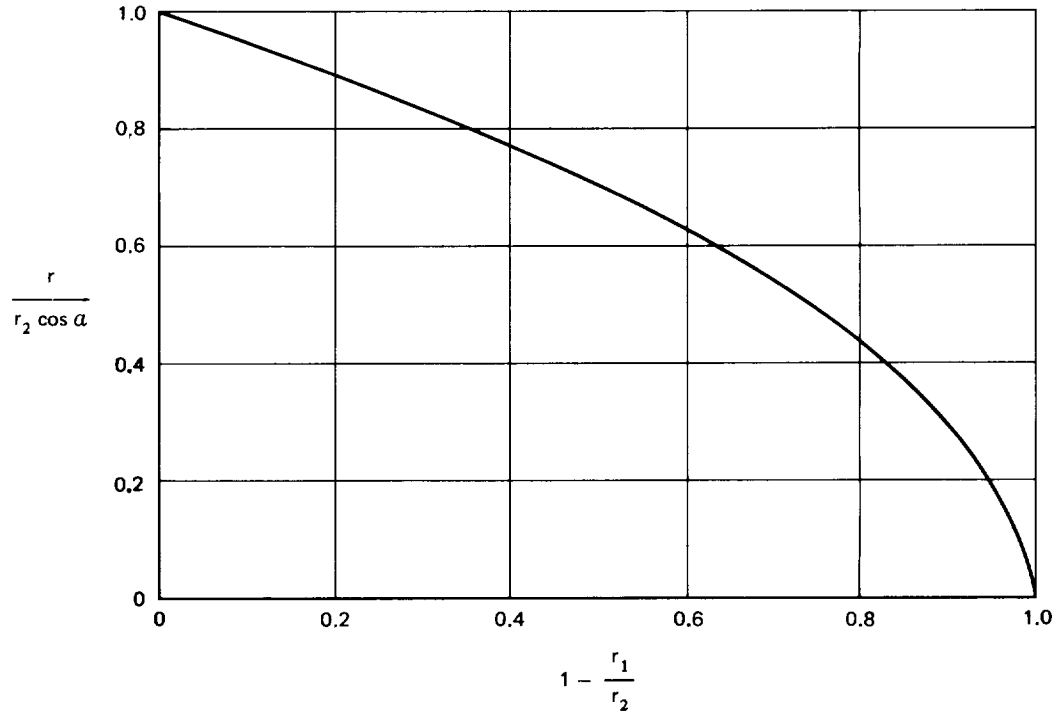

Figure 1
Variation of radius parameter with taper ratio

Theory and experiment agree for cones in torsion about as closely as they agree for cylinders in torsion (refs. 8, 12, 14, and 15). For design purposes, it is recommended that the torsional-moment coefficient in equation (11) be taken as

$$\gamma = 0.67 \tag{12}$$

No data are available for the plastic buckling of conical shells in torsion. The plasticity factor used for cylindrical shells in torsion should, however, give conservative results.

Thus, Young's modulus, E, is replaced by the secant modulus, E_{sec}, in equation (11). The secant modulus, E_{sec}, is obtained from a uniaxial stress-strain curve for a stress σ_N

$$\sigma_N = 2\tau_{cr} \tag{13}$$

where the value of τ_{cr} is the critical shear stress at the small end of the cone, given by

$$\tau_{cr} = \frac{T_{cr}}{2\pi r_1^2 t} \tag{14}$$

4.2.5 Combined Loads

4.2.5.1 Pressurized Conical Shells in Axial Compression

Theory for predicting buckling of internally pressurized conical shells under axial compression (ref. 16) differs from that for cylindrical shells in two respects. First, the axial load-carrying capacity is a function of internal pressure, and exceeds the sum of the load-carrying capacity of the unpressurized shell and the pressure load at the small end of the cone. Second, results of analyses for conical shells indicate that edge conditions at the small end have significant effect on the axial load-carrying capacity. The results are independent of edge conditions at the large end for long cones. No general expression can be given for the theoretical interaction curves.

Results of experiments on pressurized cones generally agree with theory when the internal-pressure parameter $\frac{p}{E}\left(\frac{r_1}{t \cos \alpha}\right)^2$ is of the order of unity or greater. For lower values of the internal-pressure parameter, there is a transition from those values to the experimental results for unpressurized, or lightly pressurized, conical shells which buckle at loads considerably below the theoretical values.

There are, however, insufficient data to warrant use of the entire increase in load-carrying capacity of internally pressurized conical shells in design. It is therefore recommended that the critical axial compressive load for a pressurized conical shell be determined by adding the pressurization load at the small end of the cone $\pi r_1^2 p$ to the compressive buckling load of the conical shell. Then

$$P_{cr} = \left[\frac{\gamma}{\sqrt{3(1-\mu^2)}} + \Delta\gamma\right](2\pi E t^2 \cos^2 \alpha) + \pi r_1^2 p \tag{15}$$

The unpressurized compressive-buckling coefficient γ is equal to 0.33 and the increase in buckling coefficient $\Delta\gamma$ for the equivalent cylindrical shell is given in figure 2. The critical axial load may be increased above the value given in equation (15), however, if the increase is substantiated by test.

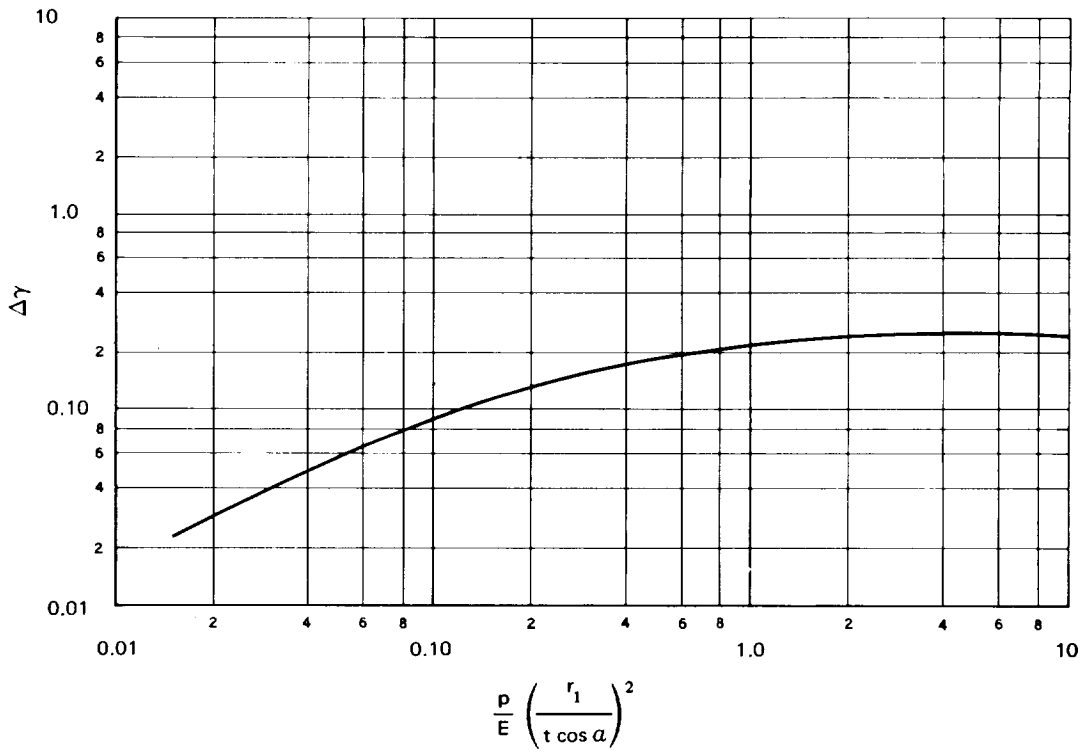

Figure 2

Increase in axial-compressive buckling-stress coefficient of conical shells due to internal pressure

4.2.5.2 Pressurized Conical Shells in Bending

As in the case of unpressurized conical shells subjected to pure bending, no theory has yet been developed for pressurized conical shells under bending. Some experiments using Mylar as the specimen material can be found in reference 8. The lack of data for materials other than Mylar does not permit the effects of plasticity to be assessed. For conservative design, therefore, the design moment of the pressurized conical shell is written as

$$M_{press} = \left[\frac{\gamma}{\sqrt{3(1-\mu^2)}} + \Delta\gamma\right] \pi E r_1 (t \cos a)^2 + \frac{p\pi r_1^3}{2} \qquad (16)$$

The unpressurized compressive buckling coefficient γ is equal to 0.41 and the increase in buckling coefficient $\Delta\gamma$ for the equivalent cylindrical shell can be obtained from figure 2. The design-critical moment for a pressurized conical shell may be increased if the increase is substantiated by test.

4.2.5.3 Combined Axial Compression and Bending for Unpressurized and Pressurized Conical Shells

Some experimental interaction curves have been obtained for unpressurized and pressurized conical shells under combined axial compression and bending (ref. 8). These investigations indicate that the following straight-line interaction curve for conical shells is adequate for design purposes:

$$R_c + R_b = 1 \tag{17}$$

where

$$R_c = \frac{P}{P_{cr}} \tag{18a}$$

and

$$R_b = \frac{M}{M_{cr}} \tag{18b}$$

For equations (18a) and (18b),

P = applied compressive load

P_{cr} = critical compressive load for cone not subjected to bending, obtained from equations (1) and (2) for unpressurized shells, and from equation (15) for pressurized shells

M = applied bending moment

M_{cr} = critical moment for cone not subjected to axial compression, as obtained from equations (5) and (6) for unpressurized shells, and from equation (16) for pressurized shells.

If actual test values of P_{cr} and M_{cr} are used, the straight-line interaction curve may no longer be conservative and the entire interaction curve must be substantiated by test.

4.2.5.4 Combined External Pressure and Axial Compression

For the conical shell subjected to combined external pressure and axial compression, a theoretical solution (ref. 17) predicts that the interaction curve for these loads deviates slightly from a straight line, with the amount of deviation depending primarily on the taper ratio of the cone. The adequacy of a straight-line interaction curve is also indicated by the few experiments reported in reference 8. Thus, the relationship

$$R_c + R_p = 1 \tag{19}$$

is recommended for design purposes. In equation (19)

$$R_p = \frac{p}{p_{cr}} \tag{20}$$

where p_{cr} is given by equations (7) and (8), and R_c is given by equation (18a).

For conical shells that buckle under combinations of external pressure and axial load so that the compressive load is near the critical axial compressive load, buckling and collapse are synonymous. As the axial load decreases and the pressure increases, experiments (ref. 11) indicate that buckling and collapse loads no longer coincide, but differ by amounts which depend on the semivertex angle of the conical shell. When the external buckling pressure is applied, for example, the axial load can be increased to a significant percentage of the critical axial compressive load before the shell collapses. Similarly, with no axial load applied, the applied external pressure can be considerably greater than the buckling pressure before the conical shell collapses. The collapse-load results were obtained for Mylar conical shells, however, and cannot be considered representative of those for metal cones. Metal cones would probably collapse at considerably lower combined loads because of the difference in plasticity properties of the materials.

4.2.5.5 Combined Torsion and External Pressure or Axial Compression

Theoretical analysis for conical shells under torsion and external hydrostatic pressure (ref. 18) indicates that the shape of the interaction curve depends on the value of the taper ratio of the cone. The limited experimental data available (refs. 18 and 19) indicate, however, that the scatter about these theoretical curves is considerable. A lower bound for the data is a straight-line interaction curve. For design purposes, the recommended interaction formula is

$$R_t + R_p = 1 \tag{21}$$

with

$$R_t = \frac{T}{T_{cr}} \tag{22}$$

where T_{cr} is given by equations (11) and (12), and R_p is given by equation (20).

For conical shells under torsion and axial compression (ref. 15), the theoretical interaction curve is nearly a straight line, while the average experimental interaction curve is parabolic in shape. The scatter of the test results, however, is such that a lower-bound straight-line interaction formula is recommended for design. Thus, for conservative design

$$R_t + R_c = 1 \tag{23}$$

where R_t is given by equation (22) and R_c by equation (18a).

4.3 Orthotropic Conical Shells

The theory of buckling of orthotropic conical shells is valuable in determining adequate buckling criteria for shells which are geometrically orthotropic because of closely spaced meridional or circumferential stiffening, as well as for shells constructed of a material whose properties differ in the two directions. An extension of the Donnell-type isotropic conical shell theory to conical shells with material orthotropy is given in reference 20, while buckling of conical shells with geometric orthotropy is considered in reference 21. Numerical results are limited to only a few values of the many parameters, but these provide the basis for tentative generalizations. Few experiments have been conducted. Following are the design recommendations based on the limited data available.

4.3.1 Uniform Hydrostatic Pressure

4.3.1.1 Constant-Thickness Orthotropic Material

A limited investigation (ref. 22) indicates that the relationship between the theoretical buckling pressures of an orthotropic conical shell and of the so-called equivalent orthotropic cylinder is similar to that for the buckling pressures of an isotropic conical shell and of the equivalent isotropic cylinder. In both cases the equivalent cylinder is

defined as one having a length equal to the slant length, L, of the conical shell, a radius equal to the average radius of curvature, $\bar{\rho}$, of the conical shell, and the same thickness. Thus, the theoretical hydrostatic buckling pressures for supported moderate-length orthotropic conical shells (refs. 23 and 24) can be expressed as

$$p_{cr} = \frac{0.86\,\gamma}{(1-\mu_s\mu_\theta)^{\frac{3}{4}}} E_s^{\frac{1}{4}} E_\theta^{\frac{3}{4}} \left(\frac{\bar{\rho}}{L}\right)\left(\frac{t}{\bar{\rho}}\right)^{\frac{5}{2}} \tag{24}$$

which reduces to the corresponding expression for the isotropic cone when we put

$$E_s = E_\theta = E$$

$$\mu_s = \mu_\theta = \mu \tag{25}$$

The theoretical value of γ is greater than unity, and depends on the ratio of end radii, as for isotropic cones.

Only limited experimental data exist for conical shells constructed of an orthotropic material (ref. 25). In the absence of a more extensive range of test results, it is recommended that the value of the correlation coefficient γ be taken as 0.75 for both orthotropic and isotropic shells.

4.3.1.2 Stiffened Conical Shells

The stability of conical shells stiffened by rings under uniform hydrostatic pressure has also been investigated (refs. 21 and 26). In these investigations, all rings were assumed to have the same cross-sectional shape and area but could have variable spacing. The approximate buckling formulas given in these references are not recommended for use in design until a larger amount of substantiating test data become available.

4.3.2 Torsion

4.3.2.1 Constant-Thickness Orthotropic Material

The investigation reported in reference 27 indicates that the theoretical buckling torque of an orthotropic conical shell is approximated by that for an equivalent orthotropic cylinder having a length equal to the height, ℓ, of the conical shell, and having the same thickness and radius given by equation (11a).

The variation of $\frac{r}{r_2 \cos \alpha}$ with $1-\frac{r_1}{r_2}$ is plotted in figure 1.

The critical torque of a moderate-length orthotropic conical shell may then be approximated by the expression

$$T_{cr} = 4.57\ \gamma\ \frac{E_\theta^{\frac{5}{8}} E_s^{\frac{3}{8}} r^2 t}{(1-\mu_\theta \mu_s)^{\frac{5}{8}}} \left(\frac{t}{r}\right)^{\frac{5}{4}} \left(\frac{r}{\ell}\right)^{\frac{1}{2}} \tag{26}$$

A reduction factor of $\gamma = 0.67$ (the value given for isotropic conical shells) is recommended. The few data points available for fiberglass-reinforced epoxy conical shells (ref. 25) yield a larger value of γ, but fall within the scatter band for the isotropic shell of constant thickness.

4.3.2.2 Ring-Stiffened Conical Shells

Although no accurate theoretical calculations have been made for ring-stiffened conical shells in torsion, a few tests (ref. 25) indicate that when the rings are equally spaced and have the same cross-sectional shape and area, a procedure similar to that for the materially orthotropic conical shell will yield adequate results. The critical torque of such a ring-stiffened conical shell may thus be approximated by the critical torque of a ring-stiffened cylinder having the radius, length, and thickness described above. The critical torque of a ring-stiffened cone with uniformly spaced rings is then given by

$$T_{cr} = 4.57\ \gamma\ \frac{Er^2 t}{(1-\mu_s \mu_\theta)^{\frac{5}{8}}} \left(\frac{t}{r}\right)^{\frac{5}{4}} \left(\frac{r}{\ell}\right)^{\frac{1}{2}} (1+\eta_0)^{\frac{5}{8}} \tag{27}$$

where (fig. 3)

$$\eta_0 = 12\ (1-\mu^2)\ \frac{E_r}{E} \left[\frac{I_r}{L_0 t^3} + \frac{A_r}{L_0 t} \left(\frac{\bar{z}_r - e_r}{t}\right)^2\right] + 12 \left(\frac{e_r}{t}\right)^2 \tag{28}$$

and the factor γ is recommended to be taken equal to 0.67. The few available test results also indicate a larger value of γ, but these again fall within the scatter band for the isotropic conical shell of constant thickness.

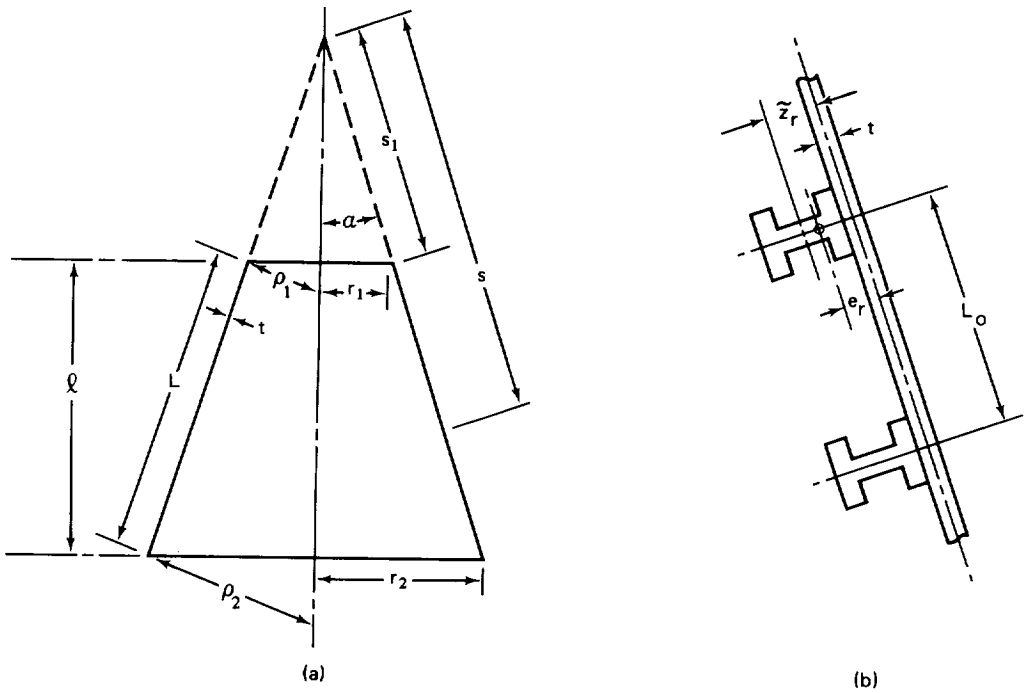

Figure 3
Notation for ring-stiffened conical shells

4.4 Sandwich Conical Shells

Neither theoretical nor experimental data are available for sandwich conical shells. If, however, the sandwich core is resistant to transverse shear so that its shear stiffness can be assumed to be infinite, the previous results for isotropic and orthotropic conical shells may readily be adapted to the analysis of sandwich conical shells by the following method.

4.4.1 Isotropic Face Sheets

If the core is assumed to have infinite transverse shear stiffness and no load-carrying capacity in the meridional or circumferential directions, the analysis for isotropic conical shells of constant thickness may be used for isotropic sandwich conical shells of constant thickness. An equivalent modulus and thickness must be defined for the sandwich shell. The face sheets may be of different thicknesses and of different materials, subject to the restriction that the Poisson's ratio of the two materials is identical. If the stretching and bending stiffnesses of such an isotropic sandwich shell

are equated to the stretching and bending stiffnesses of an equivalent constant-thickness isotropic shell having the same neutral surface dimensions, we have

$$\bar{E}\bar{t} = E_1 t_1 + E_2 t_2 \tag{29a}$$

$$\frac{\bar{E}(\bar{t})^3}{12} = \frac{h^2}{\frac{1}{E_1 t_1} + \frac{1}{E_2 t_2}} \tag{29b}$$

Then the modulus and the thickness of the equivalent constant-thickness isotropic shell are

$$\bar{t} = \frac{\sqrt{12}\, h}{\sqrt{\frac{E_1 t_1}{E_2 t_2}} + \sqrt{\frac{E_2 t_2}{E_1 t_1}}} \tag{30a}$$

$$\bar{E} = \frac{E_1 t_1 + E_2 t_2}{\bar{t}} \tag{30b}$$

The buckling loads of the isotropic sandwich shell may now be taken as the buckling loads of the equivalent isotropic shell of constant thickness as listed below.

Load	Refer to Section
Axial compression	4.2.1
Bending	4.2.2
Uniform hydrostatic pressure	4.2.3
Torsion	4.2.4
Pressurized conical shells in axial compression	4.2.5.1

Pressurized conical shells in bending	4.2.5.2
Combined axial compression and bending for unpressurized and pressurized conical shells	4.2.5.3
Combined external pressure and axial compression	4.2.5.4
Combined torsion and external pressure or axial compression	4.2.5.5

In the absence of experimental data, the reduction or correlation factors for isotropic shells of constant thickness are recommended for isotropic sandwich shells.

4.4.2 Orthotropic Face Sheets

If the core is assumed to have infinite transverse shear stiffness and no load-carrying capacity in the meridional or circumferential directions, the available results for conical shells of constant-thickness orthotropic material may be used for sandwich conical shells having orthotropic faces. The face sheets may be of different thicknesses but of the same orthotropic material so long as their principal axes are oriented in the same direction. The same procedure as for sandwich shells having isotropic face sheets leads to the following thickness and material properties of the equivalent materially orthotropic conical shells of constant thickness:

$$\bar{t} = \frac{\sqrt{12}\,h}{\sqrt{\frac{t_1}{t_2}} + \sqrt{\frac{t_2}{t_1}}} \tag{31a}$$

$$\frac{\bar{E}_s}{E_s} = \frac{\bar{E}_\theta}{E_\theta} = \frac{\bar{G}}{G} = \frac{t_1 + t_2}{\bar{t}} \tag{31b}$$

$$\frac{\bar{\mu}_s}{\mu_s} = \frac{\bar{\mu}_\theta}{\mu_\theta} = 1 \tag{31c}$$

The buckling load of the orthotropic sandwich conical shell is then the buckling load of the equivalent conical shell of orthotropic material having constant thickness. The

reduction or correlation factors for isotropic shells of constant thickness are recommended for use for sandwich shells with orthotropic face sheets.

4.4.3 Local Failure

Thus far, only overall buckling has been considered as a criterion of failure. Other modes of failures are possible, however. For honeycomb-core sandwich shells, failure may occur because of core crushing, intracell buckling, and face wrinkling. The use of relatively heavy cores ($\delta > 0.03$) will usually insure against core crushing. Lighter cores may prove to be justified as data become available. No studies have been conducted that predict localized buckling failures under stress states that are a function of position. If we assume, however, that the stress state varies only slightly over the buckled region, the following approximate equations developed for cylindrical shells can be used to predict failure from intracell buckling and face wrinkling of heavy honeycomb-core sandwich conical shells with equal-thickness face sheets under uniaxial loading. For intracell buckling

$$\sigma_s = 2.5E_R\left(\frac{t_f}{S}\right)^2 \tag{32}$$

where S is the core cell size expressed as the diameter of the largest inscribed circle and

$$E_R = \frac{4E_fE_{tan}}{\left(\sqrt{E_f} + \sqrt{E_{tan}}\right)^2} \tag{33}$$

where E_f and E_{tan} are the elastic and tangent moduli of the face-sheet material. If initial dimpling is to be checked, the equation

$$\sigma_s = 2.2E_R\left(\frac{t_f}{S}\right)^2 \tag{34}$$

should be used. The sandwich will still carry loads if initial dimpling occurs. For wrinkling

$$\sigma_s = 0.50\ (E_{sec}E_zG_{sz})^{\frac{1}{3}} \tag{35}$$

where E_z is the modulus of the core in a direction perpendicular to the core and G_{sz} is the transverse shear modulus of the core. If biaxial compressive stresses are applied to the sandwich, then the coefficients of equations must be reduced by the factor $(1 + f^3)^{-\frac{1}{3}}$ where f is the ratio of minimum to maximum principal compressive stress in face sheets.

Wrinkling and intracell-buckling equations which consider strength of bond, strength of foundation, and initial waviness of the face sheets are given in references 28, 29, and 30.

The plasticity correction factor given by equation (3) for isotropic conical shells in axial compression may be applied also to isotropic sandwich conical shells. The factor is applicable to sandwich cylinders with stiff cores and becomes somewhat conservative as the shear stiffness of the core is decreased (ref. 31).

REFERENCES

1. Almroth, B. O.; Bushnell, D.; and Sobel, L. H.; Buckling of Shells of Revolution With Various Wall Constructions. Vols. I, II, and III. NASA CR-1049-1051, 1968.

2. Ball, R. E.: A Geometrically Nonlinear Analysis of Arbitrarily Loaded Shells of Revolution. NASA CR-909, 1968.

3. Seide, P.: Axisymmetric Buckling of Circular Cones Under Axial Compression. J. Appl. Mech., vol. 23, no. 4, Dec. 1956, pp. 625-628.

4. Weingarten, V. I.; Morgan, E. J.; and Seide, P.: Elastic Stability of Thin-Walled Cylindrical and Conical Shells Under Axial Compression. AIAA J., vol. 3, no. 3, Mar. 1965, pp. 500-505.

5. Hausrath, A. H.; and Dittoe, F. A.: Development of Design Strength Levels for the Elastic Stability of Monocoque Cones Under Axial Compression. Collected Papers on Instability of Shell Structures, NASA TN D-1510, 1962, pp. 45-56.

6. Gerard, G.; and Becker, H.: Handbook of Structural Stability. Part III, Buckling of Curved Plates and Shells. Supplement to NACA TN 3783, 1957.

7. Seide, P.; and Weingarten, V. I.: On the Buckling of Circular Cylindrical Shells Under Pure Bending. J. Appl. Mech., vol. 28, no. 1, Mar. 1961, pp. 112-116.

8. Seide, P.; Weingarten, V. I.; and Morgan, E. J.: Final Report on Development of Design Criteria for Elastic Stability of Thin Shell Structures. Rept. TR-60-0000-19425 (AFBMD-TR-61-7), Space Technology Laboratories, Dec. 31, 1960.

9. Seide, P.: On the Buckling of Truncated Conical Shells Under Uniform Hydrostatic Pressure. Proc. IUTAM Symposium on the Theory of Thin Elastic Shells, Delft, The Netherlands, Aug. 24-28, 1959, North-Holland Publishing Co., The Netherlands, 1960, pp. 363-388.

10. Batdorf, S. B.: A Simplified Method of Elastic-Stability Analysis for Thin Cylindrical Shells. NACA Rept. 874, 1947.

11. Weingarten, V. I.; and Seide, P.: Elastic Stability of Thin-Walled Cylindrical and Conical Shells Under Combined External Pressure and Axial Compression. AIAA J., vol. 3, no. 5, May 1965, pp. 913-920.

12. Singer, J.; and Eckstein, A.: Recent Experimental Studies of Buckling of Conical Shells Under Torsion and External Pressure. Fifth Israel Conference, Aviation and Astronautics, Feb. 1963, pp. 135-146.

13. Seide, P.: On the Buckling of Truncated Conical Shells in Torsion. J. Appl. Mech., vol. 29, no. 2, June 1962, pp. 321-328.

14. Weingarten, V. I.: Stability of Internally Pressurized Conical Shells Under Torsion. AIAA J., vol. 2, no. 10, Oct. 1964, pp. 1782-1788.

15. Berkovits, A.; and Singer, J.: Buckling of Unstiffened Conical Shells Under Combined Torsion and Axial Compression or Tension. Seventh Israel Conference, Aviation and Astronautics, Feb. 1965, Israel Journal of Technology, vol. 3, no. 1, 1965, pp. 15-24.

16. Seide, P.: On the Stability of Internally Pressurized Conical Shells Under Axial Compression. Proc. Fourth U.S. National Congress of Applied Mechanics, University of California Press, Berkeley, California, pp. 761-773, 1962.

17. Seide, P.: Calculations for the Stability of Thin Conical Frustums Subjected to External Uniform Hydrostatic Pressure and Axial Loads. J. Aero. Sci., vol. 29, no. 8, Aug. 1962, pp. 951-955.

18. Singer, J.; and Baruch, M.: Buckling of Circular Conical Shells Under Combined Torsion and External Pressure. Topics in Applied Mechanics, Elsevir Publishing Co., Amsterdam, p. 65,1965.

19. Singer, J.: On Experimental Techniques for Interaction Curves of Buckling of Shells. Experimental Mechanics, vol. 4, no. 9, Sept. 1964, p. 279.

20. Singer, J.: Donnell-Type Equations for Bending and Buckling of Orthotropic Conical Shells. J. Appl. Mech., vol. 30, no. 2, June 1963, pp. 303-305.

21. Baruch, M.; and Singer, J.: General Instability of Stiffened Circular Conical Shells Under Hydrostatic Pressure. TAE Rept. 28, Technion-Israel Inst. of Technology, June 1963.

22. Singer, J.; and Fersht-Scher, R.: Buckling of Orthotropic Conical Shells Under External Pressure. Aeron. Quart., vol. 15, pt. 2, May 1964, p. 151.

23. Stein, M.; and Mayers, J.: A Small-Deflection Theory for Curved Sandwich Plates, NACA Rept. 1008, 1951.

24. Becker, H.; and Gerard, G.: Elastic Stability of Orthotropic Shells. J. Aeron. Sci., vol. 29, no. 5, May 1962, pp. 505-512, 520.

25. Singer, J.: On the Buckling of Unstiffened Orthotropic and Stiffened Conical Shells. Seventh International Congress for Aeronautics, Paris. June 14-16, 1965.

26. Baruch, M.; Singer, J.; and Marari, O.: Instability of Conical Shells with Non-Uniformly Spaced Stiffeners Under Hydrostatic Pressure. Seventh Israel Conference, Aviation and Aeronautics, vol. 3, no. 1, Feb. 1965, pp. 62-71.

27. Singer, J.; Fersht-Scher, R.; and Betser, A.: Buckling of Orthotropic Conical Shells Under Combined Torsion and External or Internal Pressure. Sixth Israel Conference, Aviation and Astronautics, Israel Journal of Technology, vol. 2, no. 1, Feb. 1964, pp. 179-189.

28. Plantema, F. J.: Sandwich Construction, The Bending and Buckling of Sandwich Beams, Plates and Shells. John Wiley & Sons, Inc., 1966.

29. Yusuff, S.: Face Wrinkling and Core Strength in Sandwich Construction. J. Roy. Aeron. Soc., vol. 64, no. 591, Mar. 1960, pp. 164-167.

30. Harris, B.; and Crisman, W.: Face-Wrinkling Mode of Buckling of Sandwich Panels. ASCE Journal, Engineering Mechanics Division, EM3, June 1965.

31. Peterson, J. P.: Weight-Strength Studies on Structures Representative of Fuselage Construction. NACA TN 4114, 1957.

NASA SPACE VEHICLE DESIGN CRITERIA MONOGRAPHS ISSUED TO DATE

SP-8001	(Structures)	Buffeting During Launch and Exit, May 1964
SP-8002	(Structures)	Flight-Loads Measurements During Launch and Exit, December 1964
SP-8003	(Structures)	Flutter, Buzz, and Divergence, July 1964
SP-8004	(Structures)	Panel Flutter, May 1965
SP-8005	(Environment)	Solar Electromagnetic Radiation, June 1965
SP-8006	(Structures)	Local Steady Aerodynamic Loads During Launch and Exit, May 1965
SP-8007	(Structures)	Buckling of Thin-Walled Circular Cylinders, September 1965 Revised August 1968
SP-8008	(Structures)	Prelaunch Ground Wind Loads, November 1965
SP-8009	(Structures)	Propellant Slosh Loads, August 1968
SP-8010	(Environment)	Models of Mars Atmosphere (1967), May 1968
SP-8011	(Environment)	Models of Venus Atmosphere (1968), September 1968
SP-8012	(Structures)	Natural Vibration Modal Analysis, September 1968
SP-8014	(Structures)	Entry Thermal Protection, August 1968
SP-8015	(Guidance and Control)	Guidance and Navigation for Entry Vehicles, November 1968

NASA-Langley, 1969 — 32